Short Article

Cell Metabolism

Gut-Proglucagon-Derived Peptides Are Essential for Regulating Glucose Homeostasis in Mice

Graphical Abstract

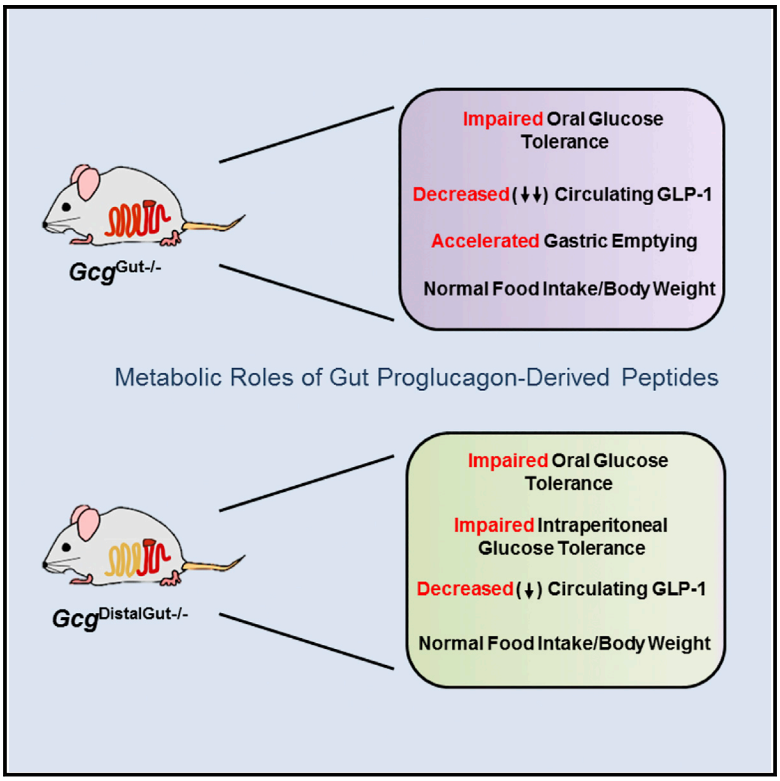

Highlights

- The mouse and human pancreas contain low levels of active GLP-1
- The gut enteroendocrine system is responsible for 95% of circulating active GLP-1
- The proximal gut sustains normal plasma GLP-1 levels in response to enteral glucose
- Gut *Gcg* expression controls glucose tolerance and gastric emptying

Authors

Youngmi Song, Jacqueline A. Koehler, Laurie L. Baggio, Alvin C. Powers, Darleen A. Sandoval, Daniel J. Drucker

Correspondence

drucker@lunenfeld.ca

In Brief

The gut-derived hormone GLP-1 also functions as an islet-derived insulinotropic peptide. Song and Koehler et al. now show that whereas the pancreas contains active GLP-1, deletion of the Gcg gene from the gut lowers circulating GLP-1, impairs glucose tolerance, and accelerates gastric emptying, highlighting essential metabolic roles of the gut GLP-1 system.

Song et al., 2019, Cell Metabolism *30*, 1–11
November 5, 2019
https://doi.org/10.1016/j.cmet.2019.08.009

CellPress

Please cite this article in press as: Song et al., Gut-Proglucagon-Derived Peptides Are Essential for Regulating Glucose Homeostasis in Mice, Cell Metabolism (2019), https://doi.org/10.1016/j.cmet.2019.08.009

Cell Metabolism
Short Article

Gut-Proglucagon-Derived Peptides Are Essential for Regulating Glucose Homeostasis in Mice

Youngmi Song,[1,2,7] Jacqueline A. Koehler,[1,7] Laurie L. Baggio,[1] Alvin C. Powers,[3,4,5] Darleen A. Sandoval,[6] and Daniel J. Drucker[1,8,*]

[1]Department of Medicine, Lunenfeld-Tanenbaum Research Institute, Mt. Sinai Hospital, University of Toronto, Toronto, ON M5G1X5, Canada
[2]Medical Research Institute, Kangbuk Samsung Hospital, Sungkyunkwan University School of Medicine, Seoul 06351, Republic of Korea
[3]Department of Medicine, Division of Diabetes, Endocrinology, and Metabolism, Vanderbilt University Medical Center, Nashville, TN 37232-0475, USA
[4]Department of Molecular Physiology & Biophysics, Vanderbilt University School of Medicine, Nashville, TN, USA
[5]Veterans Affairs Tennessee Valley Healthcare System, Nashville, TN, USA
[6]Department of Surgery, University of Michigan, Ann Arbor, MI 48105, USA
[7]These authors contributed equally
[8]Lead Contact
*Correspondence: drucker@lunenfeld.ca
https://doi.org/10.1016/j.cmet.2019.08.009

SUMMARY

The importance of pancreatic versus intestinal-derived GLP-1 for glucose homeostasis is controversial. We detected active GLP-1 in the mouse and human pancreas, albeit at extremely low levels relative to glucagon. Accordingly, to elucidate the metabolic importance of intestinal proglucagon-derived peptides (PGDPs), we generated mice with reduction of *Gcg* expression within the distal ($Gcg^{DistalGut-/-}$) or entire ($Gcg^{Gut-/-}$) gut. Substantial reduction of gut *Gcg* expression markedly reduced circulating levels of GLP-1, and impaired glucose homeostasis, associated with increased levels of GIP, and accelerated gastric emptying. $Gcg^{DistalGut-/-}$ mice similarly exhibited lower circulating GLP-1 and impaired oral glucose tolerance. Nevertheless, plasma levels of insulin remained normal following glucose administration in the absence of gut-derived GLP-1. Collectively, our findings identify the essential importance of gut-derived PGDPs for maintaining levels of circulating GLP-1, control of gastric emptying, and glucose homeostasis.

INTRODUCTION

Glucagon, a 29-amino-acid peptide, was originally identified as a hormone isolated from the pancreas with hyperglycemic activity. The molecular cloning of cDNAs and genes encoding proglucagon expanded the complexity of the proglucagon-derived peptides (PGDPs) (Drucker, 2006). Mammalian species transcribe a single proglucagon mRNA transcript yet generate a different profile of PGDPs in brain, pancreas, and intestine through tissue-specific proteolytic cleavage, mediated by members of the prohormone convertase enzyme family (Sandoval and D'Alessio, 2015). Within the pancreas, glucagon is the major liberated PGDP, and the glucagon-like peptides are contained within a larger, unprocessed major proglucagon fragment (Patzelt and Schiltz, 1984). In contrast, enteroendocrine L cells process proglucagon to liberate glicentin, oxyntomodulin, and two glucagon-like peptides: glucagon-like peptide-1 (GLP-1) and glucagon-like peptide-2 (GLP-2) (Mojsov et al., 1986).

Within the gut, two bioactive GLP-1 moieties, GLP-1(7-37), and GLP-1(7-36) amide are derived from proglucagon (Orskov et al., 1994). Both peptides circulate at low basal levels in the fasting state, are secreted rapidly following meal ingestion, and are equipotent stimulators of insulin secretion (Vahl et al., 2003). Indeed, pharmacological blockade of GLP-1 action in animals and humans, or genetic interruption of GLP-1 receptor

Context and Significance

Glucagon-like peptide 1 (GLP-1)-based drugs are effective anti-diabetic therapies. How and where GLP-1 and its related proteins are naturally produced in the body has been the topic of some debate. Investigators at the University of Michigan and University of Toronto re-examined some of their previous conclusions that the pancreas (which also produces insulin) is the main source of GLP-1 in mice. Although small amounts of active GLP-1 can be detected in both the mouse and human pancreas, disruption of the GLP-1-producing gene in the mouse gut had pronounced adverse effects on glucose control. The results reinforce the importance of gut GLP-1 secretion, physiologically and potentially pharmacologically, for control of metabolism.

signaling in mice, impairs the insulinotropic action of GLP-1, establishing the physiological importance of GLP-1 as an incretin hormone (Drucker, 2007).

Despite the preponderance of evidence demonstrating the synthesis and secretion of bioactive GLP-1 in the small and large intestine (Kreymann et al., 1988; Mojsov et al., 1986; Orskov et al., 1994), studies have also implicated pancreatic islet α cells as a source of bioactive GLP-1. Rodent and human islet cells cultured *ex vivo* secrete GLP-1 with insulinotropic activity (Ellingsgaard et al., 2011; Hansen et al., 2011; Heller and Aponte, 1995; Marchetti et al., 2012; Timper et al., 2016). Moreover, experimental pancreatic injury, including surgical manipulation, chemical damage, aging, or the prolonged nutritional stress of energy-dense diets, is associated with increased pancreatic production of GLP-1 (Kilimnik et al., 2010; Nie et al., 2000; Vasu et al., 2014).

We recently used mouse genetics and the GLP-1R antagonist exendin(9-39) to examine the consequences of selective re-induction of endogenous *Gcg* gene expression in the intestine versus the pancreas of $Gcg^{-/-}$ mice (Chambers et al., 2017). Reactivation of intestinal *Gcg* expression using the Villin-Cre system (*Gcg*$RA^{\Delta VilCre}$) restored intestinal *Gcg* and GLP-1 production, in the setting of complete loss of pancreatic *Gcg* expression (Chambers et al., 2017). Surprisingly, the GLP-1R antagonist exendin(9-39) failed to impair glycemic excursions to both oral and intraperitoneal (i.p.) glucose loads in *Gcg*$RA^{\Delta VilCre}$ mice. In contrast, selective reactivation of pancreatic *Gcg* expression in *Gcg*$RA^{\Delta PDX1Cre}$ mice and concomitant administration of exendin(9-39) led to the impairment of glycemic excursions in both oral and i.p. glucose tolerance tests. Collectively, these observations elevated the putative importance of the pancreas as a key source for GLP-1 action (Habener and Stanojevic, 2017).

Interpretation of these findings requires careful consideration of the experimental context, namely reactivation of *Gcg* expression in $Gcg^{-/-}$ mice known to exhibit α cell hyperplasia (Hayashi et al., 2009). These conditions favor the generation of pancreatic islet GLP-1 production in dedifferentiated α cells following the reintroduction of pancreatic *Gcg* expression (Hayashi et al., 2009). Moreover, $Gcg^{-/-}$ mice may exhibit compensatory induction of islet β cell GIP expression (Fukami et al., 2013), further complicating interpretation of incretin action. Critically, the importance of pancreatic versus intestinal GLP-1 activity was inferred indirectly via the glycemic response to exendin(9-39) (Chambers et al., 2017). Since the publication of these provocative findings, several studies have demonstrated that exendin(9-39) also blocks the insulinotropic actions of glucagon at the islet GLP-1 receptor (Capozzi et al., 2019a; Svendsen et al., 2018; Zhu et al., 2019), complicating precise mechanistic attribution of glycemic responses following use of exendin(9-39).

Accordingly, we have now re-examined the metabolic importance of endogenous gut-derived PGDPs in the absence of exendin(9-39) using two new lines of mice with the elimination of *Gcg* expression in the distal gut, or throughout the small and large bowel. Our findings re-establish gut-derived PGDPs as important metabolically active peptides, highlighting the potential for both enteroendocrine cells and pancreatic islet cells to serve as sources of PGDPs with glucoregulatory action.

RESULTS

Assessment of GLP-1 and Glucagon Content in Mouse and Human Pancreas

Although GLP-1 may be detected in the pancreas in the context of pancreatic injury and inflammation (Drucker, 2013; Habener and Stanojevic, 2017), active GLP-1 was not detected in mouse pancreatic perfusate (Svendsen et al., 2018) and no extractable active GLP-1 was detectable in the normal mouse pancreas (Galsgaard et al., 2018). Hence, we re-examined levels of active GLP-1 in mouse and human pancreas. Active GLP-1 content in the pancreas of wild-type (WT) $Gcg^{+/+}$ mice, maintained on normal chow (NC) or fed a 60% high-fat diet (HFD), was extremely low but detectable (Figure 1A), several orders of magnitude lower than active GLP-1 content in the colon (Figure 1A). Moreover, the levels of active GLP-1 (liberated from a common proglucagon precursor; Figure S1) in the mouse pancreas were 20- to 30-fold lower than that of glucagon and were not different after 7 weeks of HFD feeding (Figures 1B and 1C). Similar findings were observed in *Cre* control and mice with Gcg reactivation in the pancreas (*Gcg*$RA^{\Delta PDX1Cre}$) (Chambers et al., 2017) (Figure 1D), where glucagon content greatly exceeded that of active GLP-1 in pancreas-tissue extracts (Figure 1E). In contrast, neither glucagon nor active GLP-1 was detectable in the pancreas of *Gcg*-null or intestinal *Gcg*-reactivated (Gcg$RA^{\Delta VilCre}$) mice despite abundant levels of insulin (Figure 1D).

To assess the potential for species-specific differences in pancreatic GLP-1 production, we examined the human pancreas. Active GLP-1 was also detectable in normal human pancreas extracts at levels higher than in the mouse pancreas (Figure 1F, middle panel). Levels were somewhat variable, as were both glucagon and insulin content (Figure 1F, left and right panels, respectively), most likely reflecting different numbers of islets in each sample and/or age of the respective donor (Table S1). Nevertheless, glucagon content greatly exceeded that of active GLP-1 in the human pancreas (Figures 1F and 1G). Taken together, active GLP-1 is very low, but detectable, in tissue extracts from both mouse and human pancreas, albeit at much lower levels relative to glucagon.

Generation and Characterization of $Gcg^{Gut-/-}$ and $Gcg^{DistalGut-/-}$ Mice

Our previous studies addressed the glucoregulatory activity of GLP-1 in mice with reactivation of intestinal or pancreatic proglucagon (*Gcg*) expression in $Gcg^{-/-}$ mice (Chambers et al., 2017). Interpretation of the biological importance of GLP-1 in these studies relied on exendin(9-39), a GLP-1 receptor antagonist subsequently shown to block the activity of both GLP-1 and glucagon at the pancreatic GLP-1 receptor (Capozzi et al., 2019a; Svendsen et al., 2018; Zhu et al., 2019). Accordingly, to elucidate the importance of intestinal PGDP action in the absence of exendin(9-39), we generated two new lines of mice enabling the selective loss of *Gcg* expression in the intestine. $Gcg^{flox/flox}$ mice were crossed with *Vil-Cre* mice to generate $Gcg^{Gut-/-}$ mice (Figure 2A). $Gcg^{Gut-/-}$ mice exhibited a >95% reduction in *Gcg* mRNA levels throughout the entire small intestine and colon, whereas *Gcg* mRNA transcripts in the brainstem were normal (Figure 2A). Islet histology was similar (Figure S2A) and pancreatic glucagon mRNA transcripts levels were higher

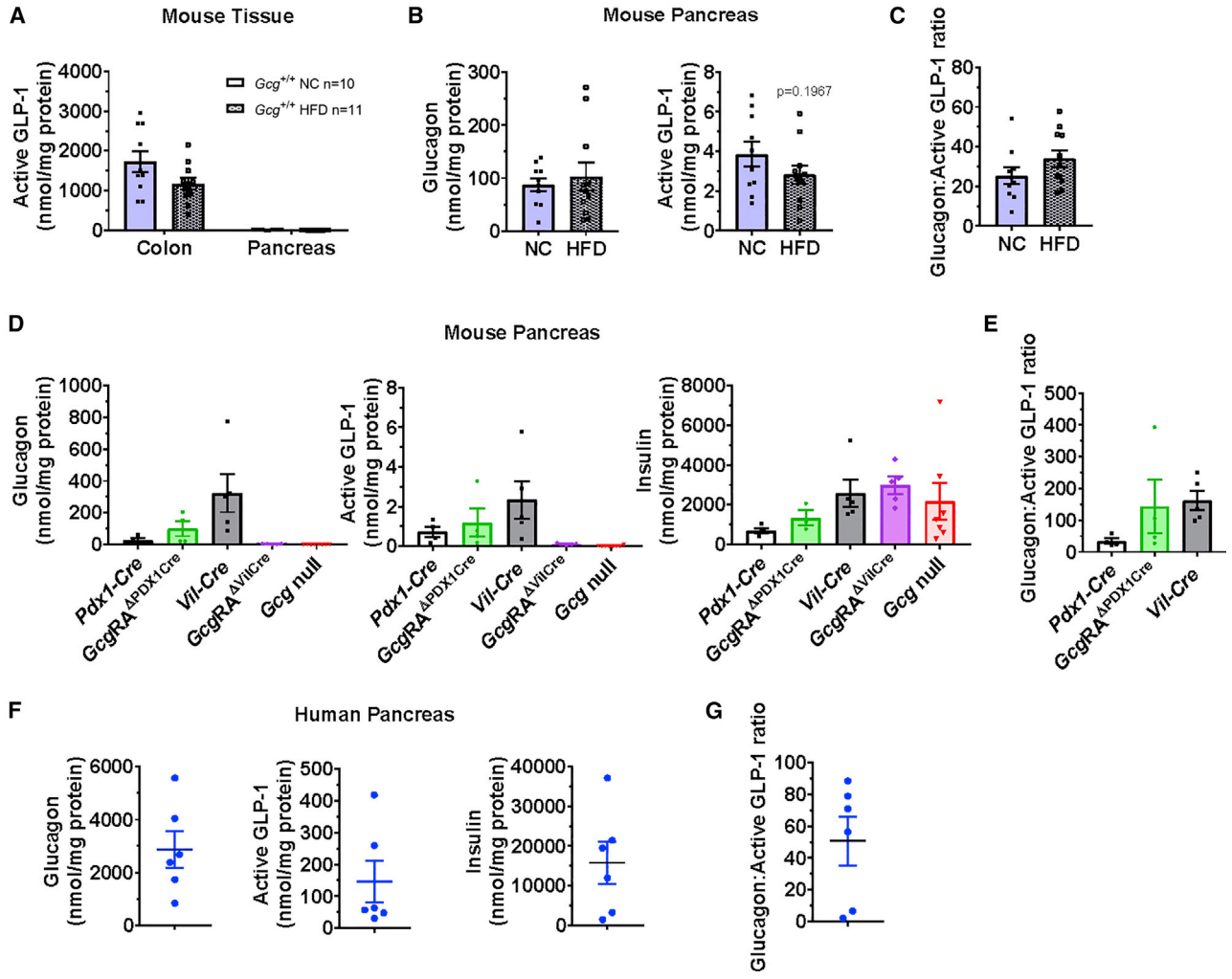

Figure 1. Assessment of Peptide Content in Mouse and Human Pancreas

(A and B) Comparison of active GLP-1 tissue levels in colon versus pancreas (A), or glucagon (left panel) and active GLP-1 tissue levels (right panel) in pancreas (B), normalized to protein content, in tissue extracts from 18- to 21-week-old WT ($Gcg^{+/+}$) male mice fed normal chow (NC) or a 60% high-fat diet (HFD) for 7 weeks.

(C) Abundance of glucagon relative to active GLP-1 (glucagon-active GLP-1 ratio) in pancreas of NC or HFD-fed mice (n = 10–11).

(D and E) Tissue levels of (D) glucagon, active GLP-1, and insulin in extracts from pancreas, normalized to protein content, and (E) relative glucagon to active GLP-1 tissue levels in pancreas of 28-week-old male *Cre* controls, *Gcg*-null, and pancreas- ($GcgRA^{\Delta PDX1Cre}$) or intestinal-reactivated ($GcgRA^{\Delta VilCre}$) mice (n = 4–5/group). For (E), glucagon:active GLP-1 ratios are not reported for $GcgRA^{\Delta VilCre}$ or *Gcg*-null mice, as glucagon and/or active GLP-1 levels were below detectable limits of the assays.

(F and G) Tissue levels of (F) glucagon, active GLP-1, and insulin in extracts from normal human pancreas, normalized to protein content, and (G) glucagon-active GLP-1 ratio in human pancreas samples (n = 6).

See also Figure S1 and Table S1.

(Figure 2A), yet pancreatic levels of active GLP-1 were very low and not different in $Gcg^{Gut-/-}$ mice (Figure 2B). Moreover, plasma levels of glucagon were similar in $Gcg^{Gut+/+}$ versus $Gcg^{Gut-/-}$ mice (Figure S2B). Consistent with the marked reduction of *Gcg* mRNA transcripts, active and total GLP-1 content was markedly reduced in all regions of the small intestine and colon from $Gcg^{Gut-/-}$ mice (Figures 2B and S2C), whereas intestinal GIP levels were not different (Figure 2C).

Despite detection of some active GLP-1 in the pancreas of both $Gcg^{Gut-/-}$ and $Gcg^{+/+}$ mice, levels were markedly lower than in the small intestine or colon of $Gcg^{+/+}$ mice (pancreas, ~6.7 pg/mg protein versus jejunum, 1,389 pg/mg protein; colon, 9,470 pg/mg protein) (Figure 2B). Similarly, relative levels of active GLP-1 remained lower in the pancreas versus the small intestine and colon of $Gcg^{Gut-/-}$ mice (pancreas, ~9.4 pg/mg protein versus jejunum, 35.5 pg/mg protein; colon, 57.7 pg/mg protein) (Figure 2B), whereas active GLP-1 levels in the pancreas of $Gcg^{+/+}$ versus $Gcg^{Gut-/-}$ mice were not different (6.7 ± 1.8 pg/mg protein versus 9.4 ± 3.2 pg/mg protein, p = 0.09). Although increased pancreatic GLP-1 production and activity have been demonstrated in the presence of metabolic stress and experimental diabetes (Kilimnik et al., 2010; Traub et al.,

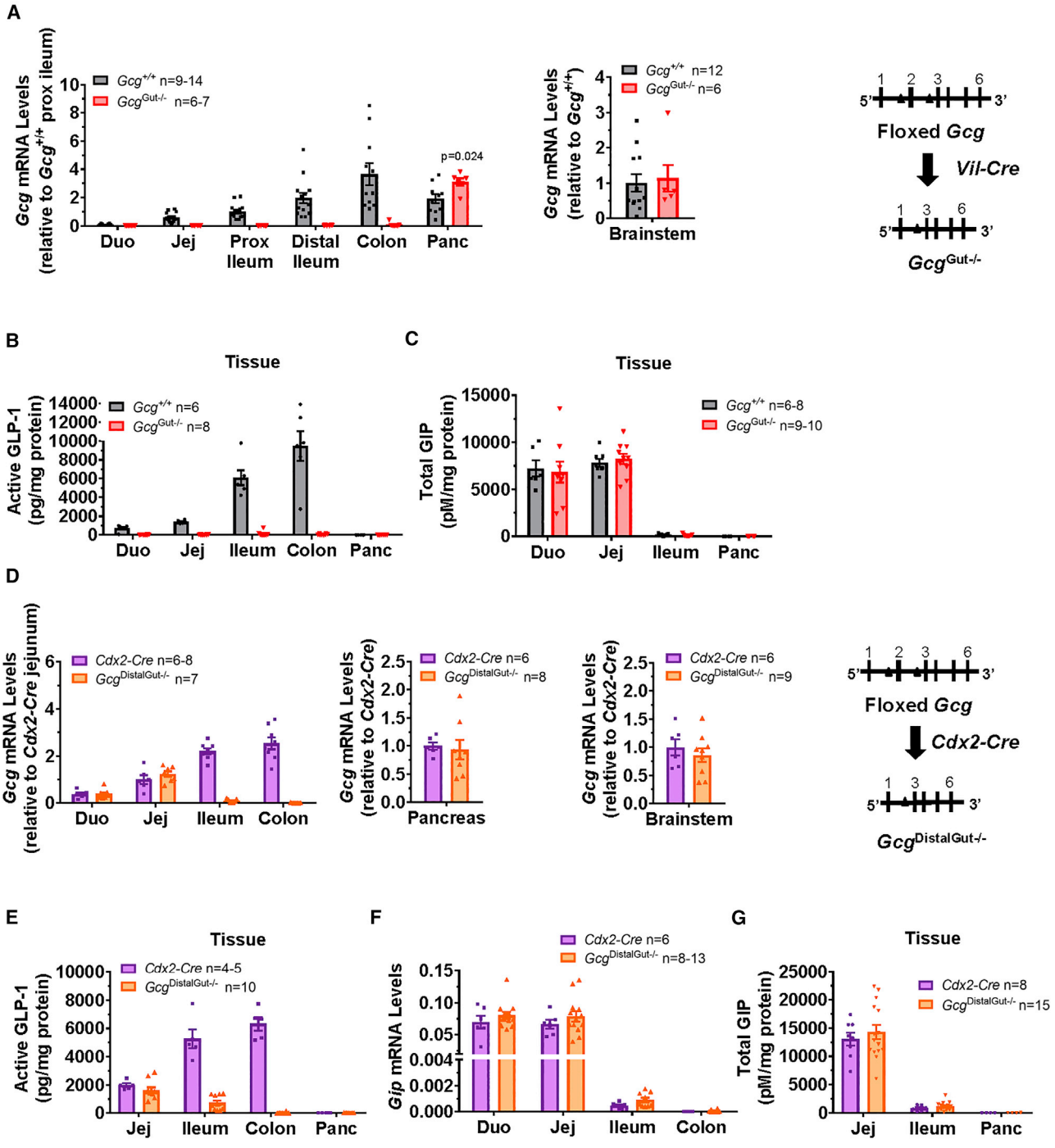

Figure 2. Characterization of $Gcg^{Gut-/-}$ and $Gcg^{DistalGut-/-}$ Mice

(A) Proglucagon (*Gcg*) mRNA abundance normalized to levels of mRNA for ribosomal protein L32 (*Rpl32*) in different regions of the small intestine, colon, and pancreas (left panel) or brainstem (right panel) of 16- to 18-week-old female mice by qPCR using a primer probe set against exons 1–2 of the *Gcg* gene (n = 6–14/group). Gene expression was expressed relative to values for *Gcg* mRNA transcripts in proximal ileum (prox ileum; left panel), or brainstem (right panel) of control $Gcg^{+/+}$ mice.

(B and C) Active GLP-1 (B) and total GIP levels (C), normalized to total protein content, in whole-tissue extracts from different regions of the intestine and pancreas of 16- to 18-week-old female mice (n = 6–8/group for GLP-1, n = 6–10 for GIP). Duo, duodenum; Jej, jejunum; Prox ileum, proximal ileum; Panc, pancreas. $Gcg^{+/+}$ mice represent combined data from WT, $Gcg^{flox/flox}$, and *Vil-Cre* control mice.

(D) *Gcg* mRNA abundance normalized to cyclophilin (*Ppia*) in different regions of the small intestine and colon (left panel), pancreas (middle panel), or brainstem (right panel) of 20- to 23-week-old male mice by qPCR (n = 6–9/group). Gene expression was expressed relative to *Gcg* mRNA levels in control (*Cdx2-Cre*) mice.

(legend continued on next page)

2017), active GLP-1 levels from pancreatic extracts of *Vil-Cre* and $Gcg^{Gut-/-}$ mice remained exceptionally low and did not increase after 7 weeks of HFD feeding (Figure S2D). In contrast to the low pancreatic levels of active GLP-1, assessment of total immunoreactive GLP-1 in the pancreas using an assay that recognizes all molecular forms of GLP-1 (Figure S1) revealed much higher levels (Figure S2C), consistent with the immunodetection of the GLP-1 sequence contained within the major proglucagon fragment (MPGF) (Patzelt and Schiltz, 1984).

We next established a second mouse model of intestinal PGDP deficiency within the distal, but not proximal gut, by crossing $Gcg^{flox/flox}$ mice with *Cdx2-Cre* mice to generate $Gcg^{DistalGut-/-}$ mice. *Gcg* mRNA transcripts were markedly reduced in the ileum and colon of $Gcg^{DistalGut-/-}$ mice, without perturbation of *Gcg* mRNA levels in the proximal small intestine, pancreas, or brainstem (Figure 2D). Both active and total GLP-1 levels were markedly reduced in the ileum and colon of $Gcg^{DistalGut-/-}$ mice; however, GLP-1 content was not reduced in the jejunum (Figures 2E and S3A). Similarly, *Gip* mRNA levels and tissue GIP content were not different in $Gcg^{DistalGut-/-}$ mice (Figures 2F and 2G).

$Gcg^{Gut-/-}$ Mice Exhibit Impaired Oral but Normal i.p. Glucose Tolerance

Despite the preservation of pancreatic *Gcg* expression in $Gcg^{Gut-/-}$ mice (Figure 2A), fasting plasma levels of total immunoreactive GLP-1 were lower in $Gcg^{Gut-/-}$ mice (Figure 3A). Moreover, fasting plasma active GLP-1 levels were markedly reduced in $Gcg^{Gut-/-}$ mice (Figure 3B), highlighting the predominant contribution of the intestine to the circulating pool of bioactive GLP-1. Conversely, although intestinal GIP levels were not different in $Gcg^{Gut-/-}$ versus $Gcg^{+/+}$ mice (Figure 2C), fasting plasma levels of GIP were higher in $Gcg^{Gut-/-}$ mice (Figure S2B) without differences in fasting levels of insulin and glucagon (Figure S2B). Remarkably, despite the importance of basal GLP-1R signaling for control of food intake and body weight (Campbell and Drucker, 2013; Patterson et al., 2011; Sandoval and D'Alessio, 2015), both incremental and cumulative food intake and body weight on regular chow and HFD were similar in $Gcg^{Gut-/-}$ versus control mice (Figures S2E and S2F). Thus, marked reductions in GLP-1 of intestinal origin have no meaningful impact on food intake and body weight.

Following an oral glucose challenge, $Gcg^{Gut-/-}$ mice exhibited higher glycemic excursions compared to *Vil-Cre* controls without differences in fasting glucose (Figures 3C and 3D). Consistent with the marked reduction of *Gcg* mRNA transcripts in the intestine, both total and active plasma GLP-1 levels did not increase following enteral glucose loading in $Gcg^{Gut-/-}$ mice but increased in $Gcg^{Gut+/+}$ mice (Figures 3E and 3F). In contrast, plasma GIP levels were higher following glucose challenge in $Gcg^{Gut-/-}$ mice than *Vil-Cre* controls (Figure 3G). Surprisingly, glucose-stimulated insulin levels and reductions in plasma glucagon were similar between $Gcg^{Gut-/-}$ and *Vil-Cre* control mice (Figures 3H and 3I). However, gastric emptying was accelerated in $Gcg^{Gut-/-}$ mice (Figure 3J). Accordingly, we bypassed the gut and administered i.p. glucose. $Gcg^{Gut-/-}$ mice exhibited glycemic excursions comparable to controls following i.p. glucose challenge (Figure 3K), without differences in plasma insulin levels (Figure 3L).

$Gcg^{DistalGut-/-}$ Mice Exhibit Impaired Oral and i.p. Glucose Tolerance

Although levels of *Gcg* mRNA transcripts and tissue content of PGDPs are higher in the distal gut (Roberts et al., 2019; van der Wielen et al., 2016), the relative importance and contribution of the proximal versus distal gut to GLP-1 secretion and action remains uncertain and controversial (Svendsen et al., 2015). In contrast to findings in $Gcg^{Gut-/-}$ mice, fasting plasma total GLP-1 levels were comparable between $Gcg^{DistalGut-/-}$ mice and controls (Figure 4A), suggesting that proximal gut *Gcg* expression contributes to circulating immunoreactive GLP-1. Strikingly, plasma levels of active GLP-1 were markedly reduced in fasted $Gcg^{DistalGut-/-}$ mice (Figure 4B), revealing the predominant contribution of distal gut *Gcg* expression to circulating bioactive GLP-1. In contrast, fasting plasma GIP, insulin, and glucagon were similar between $Gcg^{DistalGut-/-}$ mice and controls (Figure S3B), and food intake and body weight were not different in $Gcg^{DistalGut-/-}$ mice on regular chow or after several weeks of HFD feeding (Figures S3C and S3D).

Consistent with the reductions in plasma active GLP-1, $Gcg^{DistalGut-/-}$ mice exhibited oral glucose intolerance, associated with slightly higher fasting glucose levels (Figures 4C and 4D). Surprisingly, both total and active GLP-1 plasma levels increased equivalently following oral glucose challenge in $Gcg^{DistalGut-/-}$ versus *Cdx2-Cre* control mice, despite the elimination of distal gut *Gcg* expression (Figures 4E and 4F), unmasking the importance of proximal gut *Gcg* expression for the rapid rise in plasma GLP-1 levels following oral glucose. Consistent with findings in $Gcg^{Gut-/-}$ mice, GIP levels were higher after oral glucose challenge in $Gcg^{DistalGut-/-}$ versus *Cdx2-Cre* mice (Figure 4G). Despite elevated glucose excursions, glucose-stimulated insulin levels and reductions in plasma glucagon were similar between $Gcg^{DistalGut-/-}$ and *Cdx2-Cre* control mice after oral glucose challenge (Figures 4H and 4I). $Gcg^{DistalGut-/-}$ mice also exhibited modestly higher glucose excursions following an intraperitoneal glucose load; however, this was partially driven by higher fasting glucose levels (Figures 4J and 4K), and glucose-stimulated insulin levels were not different in $Gcg^{DistalGut-/-}$ versus *Cdx2-Cre* control mice (Figure 4L)

DISCUSSION

Initial concepts of GLP-1 action as a gut-derived incretin hormone stemmed from its isolation from the small and large bowel, whereas pancreatic extracts contained little bioactive intact GLP-1 (Orskov et al., 1987), and studies with perfused pancreas preparations did not detect GLP-1 in pancreatic effluents

(E) Active GLP-1 levels, normalized to total protein content, in whole-tissue extracts from different regions of the intestine and pancreas of 20- to 23-week-old male mice (n = 4–10/group).
(F) *Gip* mRNA abundance normalized to cyclophillin (*Ppia*) from different regions of the small intestine and colon of 20- to 23-week-old male mice (n = 6–13/group).
(G) Total GIP levels, normalized to total protein content, in whole-tissue extracts from the small intestine of 20- to 23-week-old male mice (n = 8–15/group).
See also Figures S2 and S3.

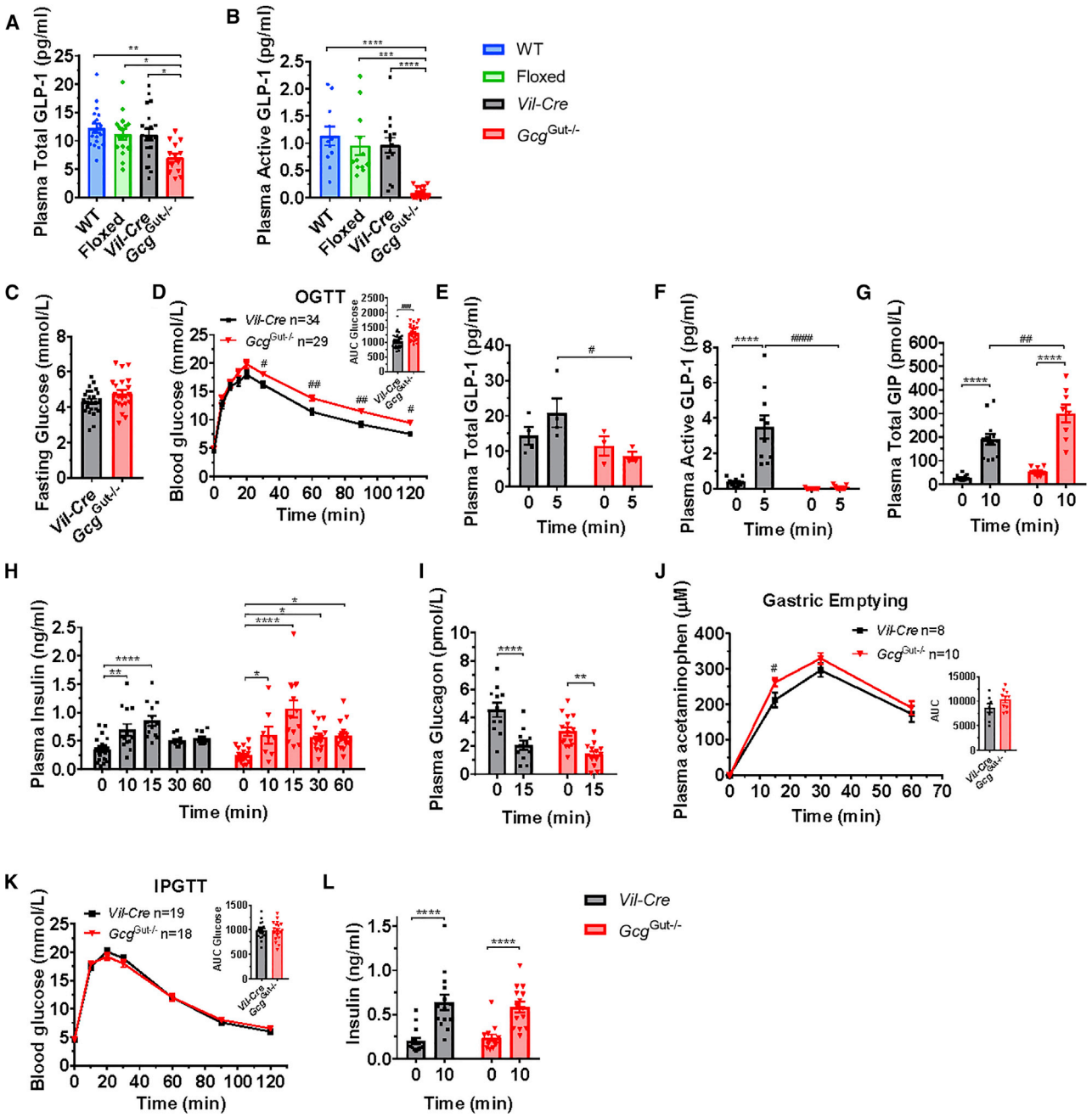

Figure 3. Loss of Gut *Gcg* Expression Produces Glucose Intolerance Following Oral, but not i.p., Glucose Administration

(A and B) Fasting plasma levels of (A) total GLP-1 or (B) active GLP-1 in overnight fasted 10- to 17-week-old male $Gcg^{Gut-/-}$ and control mice (n = 11–19/group).

(C and D) Fasting blood glucose levels (C) and blood glucose levels (D) 0–120 min after oral glucose (OGTT, 1.5g/kg) and area under the curve (AUC, inset) for glucose excursions in overnight fasted 12- to 17-week-old male $Gcg^{Gut-/-}$ and *Vil-Cre* control mice (n = 29–34/group).

(E–I) Plasma total GLP-1 (E), active GLP-1 (F), total GIP (G), insulin (H), and glucagon (I) measured before and 5–60 min after oral glucose challenge, as indicated (n = 4–15/group).

(J) Plasma acetaminophen levels, as a measurement of gastric emptying, 0–60 min after co-administration of oral acetaminophen and glucose (n = 8–10/group).

(K) Blood glucose levels before and after i.p. administration of glucose (IPGTT, 1.5 g/kg) and AUC (inset) for i.p. glucose excursions in overnight fasted 14- to 19-week-old male $Gcg^{Gut-/-}$ and *Vil-Cre* control mice (n = 19–18/group).

(L) Plasma insulin measured before and 10 min after an intraperitoneal glucose challenge (n = 14/group).

Data are presented as the mean ± SEM. (A and B) *p < 0.05, **p < 0.01, ***p < 0.001, ****p < 0.0001, control versus $Gcg^{Gut-/-}$ mice. (D–L) *p < 0.05, **p < 0.01, ****p < 0.0001, 0 versus 5–60 min. #p < 0.05, ##p<0.01, ###p < 0.001, ####p < 0.0001, $Gcg^{Gut-/-}$ versus *Vil-Cre* mice. See also Figures S2 and S4.

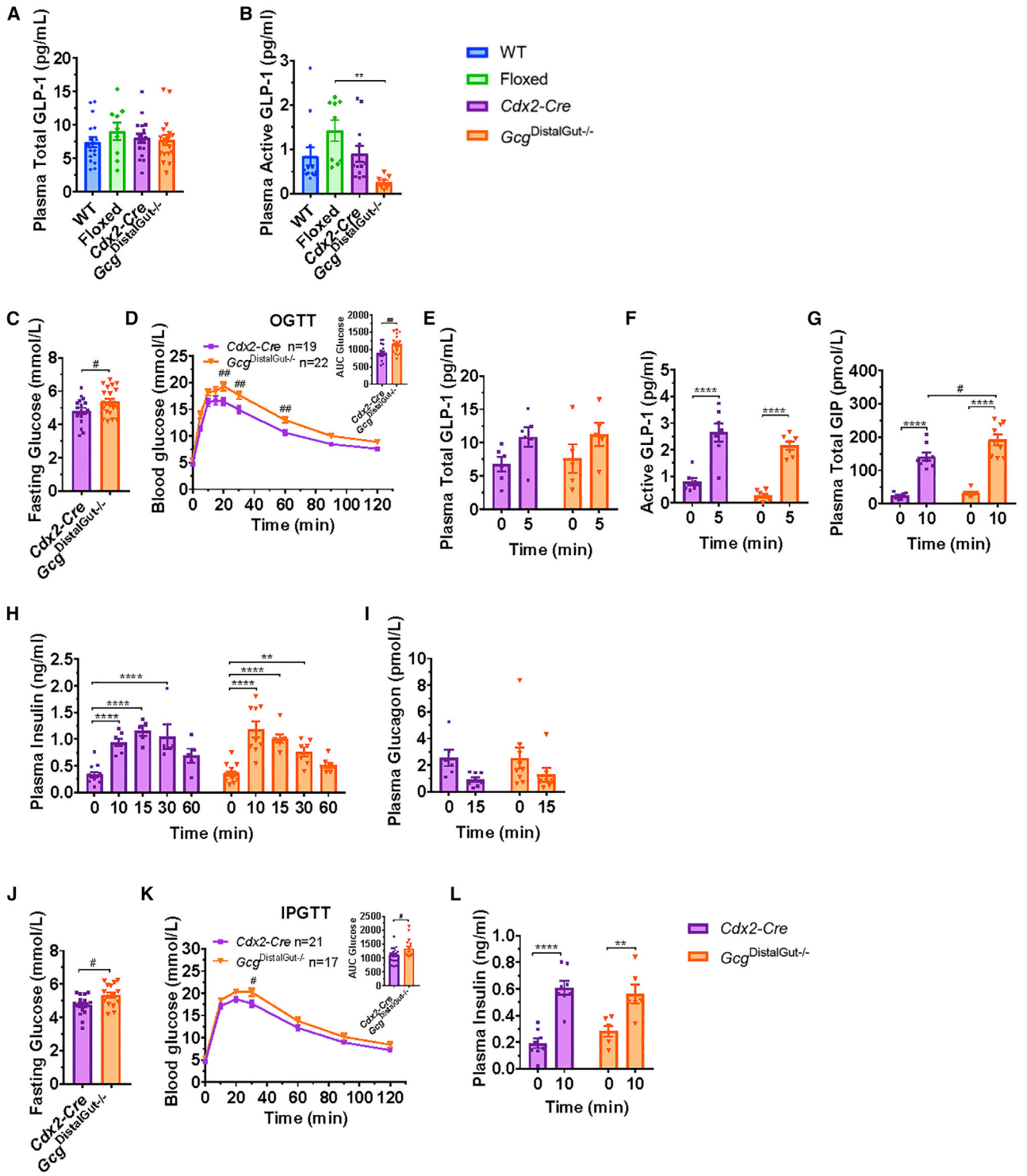

Figure 4. $Gcg^{DistalGut-/-}$ Mice Exhibit Impaired Glucose Tolerance

(A and B) Fasting plasma levels of (A) total GLP-1 or (B) active GLP-1 in overnight fasted 10- to 14-week-old male $Gcg^{DistalGut-/-}$ and control mice (n = 7–17/group).

(C and D) Fasting glucose (C) blood glucose levels (D) after oral glucose (OGTT, 1.5 g/kg) and area under the curve (AUC, inset) for glucose excursions in overnight fasted 12- to 15-week-old male $Gcg^{DistalGut-/-}$ and *Cdx2-Cre* control mice (n = 19–22/group).

(E–I) Plasma total GLP-1 (E), active GLP-1 (F), total GIP (G), insulin (H), and glucagon (I) measured before and 5–60 min after oral glucose challenge as indicated (n = 5–9/group).

(legend continued on next page)

(Orskov et al., 1986; Svendsen et al., 2018). Moreover, circulating GLP-1 levels increased briskly following oral glucose or meal ingestion, consistent with a gut-derived source for the peptide. Nevertheless, some (Mojsov et al., 1990), but not all (Galsgaard et al., 2018; Larraufie et al., 2019), studies report small amounts of GLP-1(7-36)amide in the normal rat or mouse pancreas and both pancreatic GLP-1 and *Pcsk1* expression were increased in the rat pancreas following induction of experimental diabetes with streptozotocin (Nie et al., 2000). A considerable body of subsequent evidence is now consistent with the production of islet GLP-1 in the context of experimental pancreatic inflammation, diabetes, and aging (Chen et al., 2018; Ellingsgaard et al., 2011; Habener and Stanojevic, 2017). Our current findings further support the concept of pancreatic GLP-1 production by demonstrating low but detectable levels of active GLP-1 in the mouse and human pancreas.

The studies described herein stemmed from our provocative findings revealing the importance of pancreatic PGDPs and GLP-1 (Chambers et al., 2017), motivated in part by new data confirming exendin(9-39) as a dual glucagon and GLP-1 antagonist at the GLP-1R (Capozzi et al., 2019a; Svendsen et al., 2018; Zhu et al., 2019). Using a different experimental design, Chambers et al. (2017) assessed the consequences of reactivating pancreatic or intestinal *Gcg* expression in $Gcg^{-/-}$ mice using the glycemic response to exendin(9-39) to infer the relative importance of pancreatic versus intestinal GLP-1 production. Nevertheless, multiple studies (Capozzi et al., 2019a, 2019b; Svendsen et al., 2018; Zhu et al., 2019) have recently demonstrated that (1) glucagon acts as a potential insulinotropic factor via the islet GLP-1 receptor and (2) the insulinotropic actions of glucagon are blocked by exendin(9-39).

Notably, $Gcg^{-/-}$ mice exhibit resistance to the development of glucose intolerance (Fukami et al., 2013), reflecting the absence of pancreatic glucagon, which in turn lowers hepatic glucose production. Moreover, $Gcg^{-/-}$ mice exhibit substantial pancreatic enlargement and both islet and α cell hyperplasia, further magnifying the potential contribution of islet-derived GLP-1 or glucagon produced following the re-establishment of *Gcg* expression within hyperplastic islets (Chambers et al., 2017; Hayashi et al., 2009). Furthermore, some lines of $Gcg^{-/-}$ mice exhibit upregulation of islet GIP expression (Fukami et al., 2013), additionally complicating interpretation of incretin action, insulin levels, and islet function *in vivo*.

Given these limitations, we re-examined the importance of intestinal PGDPs and GLP-1 for glucose homeostasis without the concomitant use of exendin(9-39). We generated two new mouse models using Cre driver lines targeting the epithelium, including enteroendocrine cells, in the distal or the entire gut. These two new mouse lines enabled physiological analysis of the metabolic consequences of distal ($Gcg^{DistalGut-/-}$) or virtually complete ($Gcg^{Gut-/-}$ mice) elimination of intestinal *Gcg* expression, while preserving normal pancreatic islet structure, function, and PGDP expression. Our current studies reveal the importance of gut *Gcg* expression for normal circulating levels of active GLP-1 and glucoregulation. First, plasma active GLP-1 levels were clearly reduced in both $Gcg^{Gut-/-}$ and in $Gcg^{DistalGut-/-}$ mice. Second, plasma GLP-1 levels failed to increase following oral glucose challenge in $Gcg^{Gut-/-}$ mice, providing clear proof that the gut is a key source of circulating GLP-1 following enteral nutrient ingestion. Third, loss of gut-derived PGDPs was associated with impaired oral glucose tolerance in $Gcg^{Gut-/-}$ mice and $Gcg^{DistalGut-/-}$ mice, highlighting the importance of gut PGDPs for glucose homeostasis. Collectively, these findings are consistent with substantial evidence that intestinal-derived GLP-1 acts as a circulating hormone, or locally through a gut-brain axis (Grasset et al., 2017), to control gut motility, islet hormone secretion, and glucose homeostasis.

Nevertheless, despite the loss of gut GLP-1 production and reduced glucose-stimulated levels of GLP-1 in $Gcg^{Gut-/-}$ mice, we did not detect any changes in food intake and body weight or any reduction of glucose-stimulated insulin levels following the oral glucose challenge. Notably, however, $Gcg^{Gut-/-}$ mice and $Gcg^{DistalGut-/-}$ mice are unable to fully augment insulin secretion to prevent hyperglycemia in the face of an enteral glucose challenge. Another explanation for the relatively normal insulin response resides in the increased levels of GIP following oral glucose challenge in both $Gcg^{Gut-/-}$ and $Gcg^{DistalGut-/-}$ mice. It also seems likely that both pancreatic GLP-1 and glucagon may act as local glucoincretins to enhance insulin secretion in the face of reduced intestinal GLP-1 production (Capozzi et al., 2019a; Svendsen et al., 2018; Zhu et al., 2019). A notable phenotype of gut GLP-1 deficiency demonstrated herein is the acceleration of gastric emptying. This observation is consistent with an essential role for GLP-1 in the inhibitory control of basal and meal-regulated antroduodenal motility (Schirra et al., 2006; Witte et al., 2011). Collectively, these findings emphasize the essential importance of gut-derived PGDPs for control of gastric emptying and glucose homeostasis.

Considerable historical debate and controversy surround the relative abundance and importance of proximal versus distal gut L cells for the control of glucose homeostasis. Some studies have highlighted a key role for proximal-distal gut communication, wherein distal gut L cells are rapidly activated via neural and hormonal amplification signals (Lim and Brubaker, 2006). Alternatively, direct perfusion of the proximal versus distal human gut with glucose revealed a relatively greater capacity of the distal small bowel for GLP-1 secretion and acute glucose disposal (Zhang et al., 2019). Recent studies have suggested that the proximal gut may be a more important source of functionally competent L cells than originally postulated (Glass et al., 2017; Jorsal et al., 2018; Svendsen et al., 2015). Surprisingly, levels of active GLP-1 rose briskly following oral glucose administration and were not different in control versus $Gcg^{DistalGut-/-}$ mice. Hence, the proximal gut is indeed capable of mounting a brisk GLP-1 response to oral glucose despite the marked reduction of distal gut *Gcg* expression. Nevertheless,

(J and K) Fasting glucose levels (J) and blood glucose levels (K) following i.p. administration of glucose (IPGTT, 1.5 g/kg) and AUC (inset) for i.p. glucose excursions in overnight fasted 14- to 17-week-old male $Gcg^{DistalGut-/-}$ and *Cdx2-Cre* control mice.

(L) Plasma insulin before and 10 min after an i.p. glucose challenge.

For (J) and (K), n = 17–21/group and for (L), n = 6–8/group. Data are presented as the mean ± SEM. (B) **p < 0.01, control versus $Gcg^{DistalGut-/-}$ mice. (C–L) **p < 0.01, ****p < 0.0001, 0 versus 5–60 min. #p < 0.05, ##p < 0.01, $Gcg^{DistalGut-/-}$ versus *Cdx2-Cre* mice. See also Figures S3 and S4.

Gcg$^{DistalGut-/-}$ mice exhibit reduced fasting levels of circulating active GLP-1, together with impaired oral glucose tolerance. These findings buttress the importance of the distal gut as a critical source of circulating PGDPs with glucoregulatory activity.

In normal healthy mice, the relevance of pancreatic production of GLP-1 for the control of glucose homeostasis remains uncertain, in that pancreatic levels of active GLP-1 are at the lower limit of detection. In contrast, pancreatic levels of glucagon are substantially higher than those of GLP-1, and recent studies highlight the activity of islet glucagon, acting predominantly through the GLP-1 receptor, as a local regulator of insulin secretion (Capozzi et al., 2019a; Svendsen et al., 2018; Zhu et al., 2019). Taken together, our new findings integrated together with previous studies of pancreatic PGDP activity (Capozzi et al., 2019a; Chambers et al., 2017; Svendsen et al., 2018; Traub et al., 2017) emphasize the potential contributions of both the pancreas and the intestine to the generation of glucoregulatory PGDPs, and the regulation of GLP-1R-dependent insulin secretion and glucose homeostasis.

Limitations of Study

Our experimental design and findings have a number of limitations. We studied predominantly healthy mice and did not examine mice with experimental diabetes or prolonged HFD feeding and severe obesity. The new mouse lines studied here exhibit germline elimination of the *Gcg* gene; hence, we cannot rule out the possibility that one or both lines have adapted physiologically to compensate for developmental loss of gut PGDPs. Indeed, plasma levels of GIP were increased in both *Gcg*$^{Gut-/-}$ and *Gcg*$^{DistalGut-/-}$ mice. Hence, the absence of gut GLP-1 and its impact on the incretin effect were potentially modified by compensatory upregulation of GIP action, as described previously for Glp1r$^{-/-}$ and Gcg$^{-/-}$ mice (Fukami et al., 2013; Pederson et al., 1998). Notably, we detected a very small amount of active GLP-1 in mouse pancreatic extracts. Hence, we cannot rule out a role for local islet GLP-1 or glucagon action in the context of the distal or complete elimination of intestinal *Gcg* expression. Importantly, we also report variable yet consistently detectable levels of active GLP-1 in the human pancreas. Furthermore, the current study was not designed to distinguish the extent of pancreatic GLP-1 receptor activation arising from locally produced glucagon and GLP-1, versus circulating GLP-1 or oxyntomodulin produced in the gut. Nevertheless, our new findings highlight the unequivocal importance of intestinal PGDPs in the control of gut motility and the regulation of glucose homeostasis.

STAR★METHODS

Detailed methods are provided in the online version of this paper and include the following:

- KEY RESOURCES TABLE
- LEAD CONTACT AND MATERIALS AVAILABILITY
- EXPERIMENTAL MODEL AND SUBJECT DETAILS
  - Animals
- METHOD DETAILS
  - Assessment of *Gcg* Knockdown
  - Glucose Tolerance Testing
  - Metabolic Measurements
  - Pancreas Samples
  - Tissue Peptide Content
  - Gastric Emptying
  - Food Intake
  - Immunohistochemistry
- QUANTIFICATION AND STATISTICAL ANALYSIS

SUPPLEMENTAL INFORMATION

Supplemental Information can be found online at https://doi.org/10.1016/j.cmet.2019.08.009.

ACKNOWLEDGMENTS

D.J.D. is supported in part by a Novo Nordisk, Banting and Best Diabetes Center Chair in incretin biology and CIHR Foundation grant 154321. Mt. Sinai Hospital receives support for studies of incretin biology in the Drucker lab from Novo Nordisk. Y.S. is supported by a fellowship program from the BBDC and the Kangbuk Samsung Hospital. The human pancreatic specimens were collected using funding provided by the NIDDK-supported Human Islet Research Network (HIRN, RRID: SCR_014393; https://hirnetwork.org; UC4 DK104211 and DK108120), DK106755, and DK20593. We thank Rita Bottino (Allegheny Health Network, Pittsburgh, PA) for processing the human pancreata.

AUTHOR CONTRIBUTIONS

Y.S., J.A.K., L.L.B., and D.J.D. designed experiments. Y.S., J.A.K., and L.L.B. carried out experiments and analyzed data. D.A.S. provided mouse lines and reviewed and edited the paper. A.C.P. provided human pancreas samples and edited the manuscript. Y.S., J.A.K., L.L.B., and D.J.D. wrote and edited the paper. D.J.D. is the guarantor for this work and the Lead Contact.

DECLARATION OF INTERESTS

D.J.D. has served as an advisor, consultant, or speaker in the past 12 months to Forkhead Biotherapeutics, Heliome, Inc., Intarcia Therapeutics, Kallyope, Eli Lilly, Merck Research Laboratories, Novo Nordisk, Inc., Pfizer, Inc., and Sanofi, Inc. Neither D.J.D. nor his family members hold stock directly or indirectly in any of these companies.

Received: February 15, 2019
Revised: July 3, 2019
Accepted: August 9, 2019
Published: September 5, 2019

REFERENCES

Brissova, M., Haliyur, R., Saunders, D., Shrestha, S., Dai, C., Blodgett, D.M., Bottino, R., Campbell-Thompson, M., Aramandla, R., Poffenberger, G., et al. (2018). Alpha cell function and gene expression are compromised in type 1 diabetes. Cell Rep *22*, 2667–2676.

Campbell, J.E., and Drucker, D.J. (2013). Pharmacology physiology and mechanisms of incretin hormone action. Cell Metab *17*, 819–837.

Capozzi, M.E., Svendsen, B., Encisco, S.E., Lewandowski, S.L., Martin, M.D., Lin, H., Jaffe, J.L., Coch, R.W., Haldeman, J.M., MacDonald, P.E., et al. (2019a). Beta cell tone is defined by proglucagon peptides through cAMP signaling. JCI Insight *4*.

Capozzi, M.E., Wait, J.B., Koech, J., Gordon, A.N., Coch, R.W., Svendsen, B., Finan, B., D'Alessio, D.A., and Campbell, J.E. (2019b). Glucagon lowers glycemia when beta-cells are active. JCI Insight *5*.

Chambers, A.P., Sorrell, J.E., Haller, A., Roelofs, K., Hutch, C.R., Kim, K.S., Gutierrez-Aguilar, R., Li, B., Drucker, D.J., D'Alessio, D.A., et al. (2017). The role of pancreatic preproglucagon in glucose homeostasis in mice. Cell Metab *25*, 927–934.e3.

Chen, Y.C., Taylor, A.J., and Verchere, C.B. (2018). Islet prohormone processing in health and disease. Diabetes Obes. Metab *20*, 64–76.

Drucker, D.J. (2006). The biology of incretin hormones. Cell Metab *3*, 153–165.

Drucker, D.J. (2007). The role of gut hormones in glucose homeostasis. J. Clin. Invest *117*, 24–32.

Drucker, D.J. (2013). Incretin action in the pancreas: potential promise, possible perils, and pathological pitfalls. Diabetes *62*, 3316–3323.

Ellingsgaard, H., Hauselmann, I., Schuler, B., Habib, A.M., Baggio, L.L., Meier, D.T., Eppler, E., Bouzakri, K., Wueest, S., Muller, Y.D., et al. (2011). Interleukin-6 enhances insulin secretion by increasing glucagon-like peptide-1 secretion from L cells and alpha cells. Nat. Med *17*, 1481–1489.

Fukami, A., Seino, Y., Ozaki, N., Yamamoto, M., Sugiyama, C., Sakamoto-Miura, E., Himeno, T., Takagishi, Y., Tsunekawa, S., Ali, S., et al. (2013). Ectopic expression of GIP in pancreatic beta-cells maintains enhanced insulin secretion in mice with complete absence of proglucagon-derived peptides. Diabetes *62*, 510–518.

Galsgaard, K.D., Winther-Sørensen, M., Ørskov, C., Kissow, H., Poulsen, S.S., Vilstrup, H., Prehn, C., Adamski, J., Jepsen, S.L., Hartmann, B., et al. (2018). Disruption of glucagon receptor signaling causes hyperaminoacidemia exposing a possible liver-alpha-cell axis. Am. J. Physiol. Endocrinol. Metab. *314*, E93–E103.

Glass, L.L., Calero-Nieto, F.J., Jawaid, W., Larraufie, P., Kay, R.G., Göttgens, B., Reimann, F., and Gribble, F.M. (2017). Single-cell RNA-sequencing reveals a distinct population of proglucagon-expressing cells specific to the mouse upper small intestine. Mol. Metab. *6*, 1296–1303.

Grasset, E., Puel, A., Charpentier, J., Collet, X., Christensen, J.E., Tercé, F., and Burcelin, R. (2017). A specific gut microbiota dysbiosis of type 2 diabetic mice induces GLP-1 resistance through an enteric NO-dependent and gut-brain axis mechanism. Cell Metab. *25*, 1075–1090.e5.

Habener, J.F., and Stanojevic, V. (2017). Pancreas and not gut mediates the GLP-1-induced glucoincretin effect. Cell Metab *25*, 757–758.

Hansen, A.M., Bödvarsdottir, T.B., Nordestgaard, D.N., Heller, R.S., Gotfredsen, C.F., Maedler, K., Fels, J.J., Holst, J.J., and Karlsen, A.E. (2011). Upregulation of alpha cell glucagon-like peptide 1 (GLP-1) in Psammomys obesus–an adaptive response to hyperglycaemia? Diabetologia *54*, 1379–1387.

Hayashi, Y., Yamamoto, M., Mizoguchi, H., Watanabe, C., Ito, R., Yamamoto, S., Sun, X.Y., and Murata, Y. (2009). Mice deficient for glucagon gene-derived peptides display normoglycemia and hyperplasia of islet {alpha}-cells but not of intestinal L-cells. Mol. Endocrinol. *23*, 1990–1999.

Heller, R.S., and Aponte, G.W. (1995). Intra-islet regulation of hormone secretion by glucagon-like peptide-1-(7–36)amide. Am. J. Physiol. *269*, G852–G860.

Hinoi, T., Akyol, A., Theisen, B.K., Ferguson, D.O., Greenson, J.K., Williams, B.O., Cho, K.R., and Fearon, E.R. (2007). Mouse model of colonic adenoma-carcinoma progression based on somatic Apc inactivation. Cancer Res. *67*, 9721–9730.

Jorsal, T., Rhee, N.A., Pedersen, J., Wahlgren, C.D., Mortensen, B., Jepsen, S.L., Jelsing, J., Dalbøge, L.S., Vilmann, P., Hassan, H., et al. (2018). Enteroendocrine K and L cells in healthy and type 2 diabetic individuals. Diabetologia *61*, 284–294.

Kilimnik, G., Kim, A., Steiner, D.F., Friedman, T.C., and Hara, M. (2010). Intraislet production of GLP-1 by activation of prohormone convertase 1/3 in pancreatic alpha-cells in mouse models of ss-cell regeneration. Islets *2*, 149–155.

Kreymann, B., Yiangou, Y., Kanse, S., Williams, G., Ghatei, M.A., and Bloom, S.R. (1988). Isolation and characterisation of GLP-1 7–36 amide from rat intestine. Elevated levels in diabetic rats. FEBS Lett. *242*, 167–170.

Larraufie, P., Roberts, G.P., McGavigan, A.K., Kay, R.G., Li, J., Leiter, A., Melvin, A., Biggs, E.K., Ravn, P., Davy, K., et al. (2019). Important role of the GLP-1 axis for glucose homeostasis after bariatric surgery. Cell Rep. *26*, 1399–1408.e6.

Lim, G.E., and Brubaker, P.L. (2006). Glucagon-like peptide 1 secretion by the L-cell: the view from within. Diabetes *55*, S70–S77.

Maida, A., Lovshin, J.A., Baggio, L.L., and Drucker, D.J. (2008). The glucagon-like peptide-1 receptor agonist oxyntomodulin enhances {beta}-cell function but does not inhibit gastric emptying in mice. Endocrinology *149*, 5670–5678.

Marchetti, P., Lupi, R., Bugliani, M., Kirkpatrick, C.L., Sebastiani, G., Grieco, F.A., Del Guerra, S., D'Aleo, V., Piro, S., Marselli, L., et al. (2012). A local glucagon-like peptide 1 (GLP-1) system in human pancreatic islets. Diabetologia *55*, 3262–3272.

Mojsov, S., Heinrich, G., Wilson, I.B., Ravazzola, M., Orci, L., and Habener, J.F. (1986). Preproglucagon gene expression in pancreas and intestine diversifies at the level of post-translational processing. J. Biol. Chem. *261*, 11880–11889.

Mojsov, S., Kopczynski, M.G., and Habener, J.F. (1990). Both amidated and nonamidated forms of glucagon-like peptide I are synthesized in the rat intestine and the pancreas. J. Biol. Chem. *265*, 8001–8008.

Nie, Y., Nakashima, M., Brubaker, P.L., Li, Q.L., Perfetti, R., Jansen, E., Zambre, Y., Pipeleers, D., and Friedman, T.C. (2000). Regulation of pancreatic PC1 and PC2 associated with increased glucagon-like peptide 1 in diabetic rats. J. Clin. Invest *105*, 955–965.

Orskov, C., Holst, J.J., Knuhtsen, S., Baldissera, F.G.A., Poulsen, S.S., and Nielsen, O.V. (1986). Glucagon-like peptides GLP-1 and GLP-2, predicted products of the glucagon gene, are secreted separately from pig small intestine but not pancreas. Endocrinology *119*, 1467–1475.

Orskov, C., Holst, J.J., Poulsen, S.S., and Kirkegaard, P. (1987). Pancreatic and intestinal processing of proglucagon in man. Diabetologia *30*, 874–881.

Orskov, C., Rabenhøj, L., Wettergren, A., Kofod, H., and Holst, J.J. (1994). Tissue and plasma concentrations of amidated and glycine-extended glucagon-like peptide I in humans. Diabetes *43*, 535–539.

Patterson, J.T., Ottaway, N., Gelfanov, V.M., Smiley, D.L., Perez-Tilve, D., Pfluger, P.T., Tschöp, M.H., and Dimarchi, R.D. (2011). A novel human-based receptor antagonist of sustained action reveals body weight control by endogenous GLP-1. ACS Chem. Biol. *6*, 135–145.

Patzelt, C., and Schiltz, E. (1984). Conversion of proglucagon in pancreatic alpha cells: the major endproducts are glucagon and a single peptide, the major proglucagon fragment, that contains two glucagon-like sequences. Proc. Natl. Acad. Sci. USA *81*, 5007–5011.

Pederson, R.A., Satkunarajah, M., McIntosh, C.H., Scrocchi, L.A., Flamez, D., Schuit, F., Drucker, D.J., and Wheeler, M.B. (1998). Enhanced glucose-dependent insulinotropic polypeptide secretion and insulinotropic action in glucagon-like peptide 1 receptor -/- mice. Diabetes *47*, 1046–1052.

Roberts, G.P., Larraufie, P., Richards, P., Kay, R.G., Galvin, S.G., Miedzybrodzka, E.L., Leiter, A., Li, H.J., Glass, L.L., Ma, M.K.L., et al. (2019). Comparison of human and murine enteroendocrine cells by transcriptomic and peptidomic profiling. Diabetes *68*, 1062–1072.

Sandoval, D.A., and D'Alessio, D.A. (2015). Physiology of proglucagon peptides: role of glucagon and GLP-1 in health and disease. Physiol. Rev. *95*, 513–548.

Schirra, J., Nicolaus, M., Roggel, R., Katschinski, M., Storr, M., Woerle, H.J., and Göke, B. (2006). Endogenous glucagon-like peptide 1 controls endocrine pancreatic secretion and antro-pyloro-duodenal motility in humans. Gut *55*, 243–251.

Svendsen, B., Pedersen, J., Albrechtsen, N.J., Hartmann, B., Toräng, S., Rehfeld, J.F., Poulsen, S.S., and Holst, J.J. (2015). An analysis of cosecretion and coexpression of gut hormones from male rat proximal and distal small intestine. Endocrinology *156*, 847–857.

Svendsen, B., Larsen, O., Gabe, M.B.N., Christiansen, C.B., Rosenkilde, M.M., Drucker, D.J., and Holst, J.J. (2018). Insulin secretion depends on intra-islet glucagon signaling. Cell Rep *25*, 1127–1134.e2.

Timper, K., Dalmas, E., Dror, E., Rütti, S., Thienel, C., Sauter, N.S., Bouzakri, K., Bédat, B., Pattou, F., Kerr-Conte, J., et al. (2016). Glucose-dependent insulinotropic peptide stimulates glucagon-like peptide 1 production by pancreatic islets via interleukin 6, produced by alpha cells. Gastroenterology *151*, 165–179.

Traub, S., Meier, D.T., Schulze, F., Dror, E., Nordmann, T.M., Goetz, N., Koch, N., Dalmas, E., Stawiski, M., Makshana, V., et al. (2017). Pancreatic alpha cell-

derived glucagon-related peptides are required for beta cell adaptation and glucose homeostasis. Cell Rep *18*, 3192–3203.

Vahl, T.P., Paty, B.W., Fuller, B.D., Prigeon, R.L., and D'Alessio, D.A. (2003). Effects of GLP-1-(7–36)NH(2), GLP-1-(7–37), and GLP-1- (9–36)NH(2) on intravenous glucose tolerance and glucose-induced insulin secretion in healthy humans. J. Clin. Endocrinol. Metab *88*, 1772–1779.

van der Wielen, N., Ten Klooster, J.P., Muckenschnabl, S., Pieters, R., Hendriks, H.F., Witkamp, R.F., and Meijerink, J. (2016). The noncaloric sweetener rebaudioside A stimulates glucagon-like peptide 1 release and increases enteroendocrine cell numbers in 2-dimensional mouse organoids derived from different locations of the intestine. J. Nutr *146*, 2429–2435.

Vasu, S., Moffett, R.C., Thorens, B., and Flatt, P.R. (2014). Role of endogenous GLP-1 and GIP in beta cell compensatory responses to insulin resistance and cellular stress. PLoS One *9*, e101005.

Witte, A.B., Grybäck, P., Jacobsson, H., Näslund, E., Hellström, P.M., Holst, J.J., Hilsted, L., and Schmidt, P.T. (2011). Involvement of endogenous glucagon-like peptide-1 in regulation of gastric motility and pancreatic endocrine secretion. Scand. J. Gastroenterol *46*, 428–435.

Zhang, X., Young, R.L., Bound, M., Hu, S., Jones, K.L., Horowitz, M., Rayner, C.K., and Wu, T. (2019). Comparative effects of proximal and distal small intestinal glucose exposure on glycemia, incretin hormone secretion, and the incretin effect in health and Type 2 diabetes. Diabetes Care *42*, 520–528.

Zhu, L., Dattaroy, D., Pham, J., Wang, L., Barella, L.F., Cui, Y., Wilkins, K.J., Roth, B.L., Hochgeschwender, U., Matschinsky, F.M., et al. (2019). Intra-islet glucagon signaling is critical for maintaining glucose homeostasis. JCI Insight *5*.

STAR★METHODS

KEY RESOURCES TABLE

REAGENT or RESOURCE	SOURCE	IDENTIFIER
Antibodies		
insulin	Abcam	Cat# ab181547; RRID: AB_2716761
glucagon	Cell Signalling	Cat# 2760S; RRID: AB_659831
Chemicals, Peptides, and Recombinant Proteins		
acetaminophen	Sigma	Cat# A7085
Critical Commercial Assays		
Ultrasensitive Mouse Insulin ELISA	ALPCO	Cat# 80-INSMSU-E01; RRID: AB_2792981
Active GLP-1 (ver. 2)	Mesoscale	Cat# K150JWC-1
Total GLP-1 (ver. 2)	Mesoscale	Cat# K150JVC-1; RRID: AB_2801383
Total GIP	Crystal Chem	Cat# 81517
Glucagon	Mercodia	Cat# 10-1281-01; RRID: AB_2783839
Acetaminophen-L3K	Sekisui Diagnostics	Cat# 506-30
Insulin ELISA (human)	ALPCO	Cat# 80-INSHU-E01.1; RRID: AB_2801438
Experimental Models: Organisms/Strains		
B6.Cg-Tg(Vil1-cre)997Gum/J (*Vil-Cre*)	Jackson Laboratories	Cat# JAX:004586; RRID: IMSR_JAX:004586
B6.Cg-Tg(CDX2-cre)101Erf/J (*Cdx2-Cre*)	Jackson Laboratories	Cat# JAX009350; RRID: IMSR_JAX:009350
Gcg^{tm1Rsy} ($Gcg^{flox/flox}$)	Darleen Sandoval, University of Michigan	N/A
Oligonucleotides		
Proglucagon (*Gcg*)	Applied Biosystems	Cat# Mm01269053_m1
Gastric Inhibitory Polypeptide (*Gip*)	Applied Biosystems	Cat# Mm00433601_m1
Cyclophilin *(Ppia)*	Applied Biosystems	Cat# Mm02342430_g1
Ribosomal protein L32 (*Rpl32*)	Applied Biosystems	Cat# Mm02528467_g1
Software and Algorithms		
Graph Pad Prism 7	Graphpad Software	https://www.graphpad.com
Other		
Regular Chow Diet (RC)	Harlan Teklad	Cat# 2018
High Fat Diet (HFD)	Research Diets	Cat# D12492i

LEAD CONTACT AND MATERIALS AVAILABILITY

Further information and requests for resources and reagents should be directed to and will be fulfilled by the Lead Contact, Daniel Drucker. Drucker@lunenfeld.ca

EXPERIMENTAL MODEL AND SUBJECT DETAILS

Animals

All mouse experiments were approved by the Animal Care and Use Subcommittee at the Toronto Centre for Phenogenomics (TCP), Mt. Sinai Hospital and the University of Michigan animal care committee. Mice were housed up to five per cage, kept under a 12-h light/12h-dark cycle in the TCP facility, and maintained on regular chow (RC; 18% kcal from fat, 2018, Harlan Teklad, Mississauga, ON), or High Fat Diet (HFD; 60% kcal from fat, D12492i, Research Diets, New Brunswick, NJ). All mice were given free access to food and water unless otherwise indicated. All experiments were performed using age- and sex-matched littermates. B6.Cg-Tg(Vil1-cre) 997Gum/J (*Vil-Cre*) (Cat No: 004586) and B6.Cg-Tg(CDX2-cre)101Erf/J (*Cdx2-Cre*) (Cat No: 009350) mice (Hinoi et al., 2007) were obtained from Jackson Laboratories (Bar Harbor ME). Gcg^{tm1Rsy} ($Gcg^{flox/flox}$) mice, in which exon 2 of the *Gcg* gene is flanked by *loxP* sites, was provided by Darleen Sandoval (Chambers et al., 2017). To generate $Gcg^{Gut-/-}$ and $Gcg^{DistalGut-/-}$ mice, *Vil-Cre* and *Cdx2-Cre* mice were bred with $Gcg^{flox/flox}$ mice (Chambers et al., 2017), respectively. Germline deletion was minimized by restricting *Cre* expression to female breeders for the *Vil-Cre* line, and male breeders for the *Cdx2-Cre* line, and genotypes were verified by

isolating RNA and determining length of *Gcg* transcripts in relevant tissues. To control for gene dosage, breeders were heterozygous for the *Cre* gene. Intercrossing *Cre*-positive and *Cre*-negative *Gcg loxP* heterozygotes from these 2 lines resulted in 6 genotypes: wildtype mice with no *Cre* (WT), mice homozygous for the *LoxP Gcg* gene ($Gcg^{flox/flox}$)(Floxed), wildtype mice expressing Cre recombinase (*Vil-Cre* or *Cdx2-Cre*) and $Gcg^{flox/flox}$ mice expressing Cre recombinase ($Gcg^{Gut-/-}$ and $Gcg^{DistalGut-/-}$ mice). All mice were born at the expected Mendelian ratios and appeared healthy. Whenever possible, we carried out experiments in all groups of mice; no major phenotypic differences in glucose homeostasis were observed between any of the control lines (Figure S4). For the purposes of clarity, data was presented as comparisons between *Vil-Cre* or *Cdx2-Cre* control mice to $Gcg^{Gut-/-}$ and $Gcg^{DistalGut-/-}$ mice, respectively.

METHOD DETAILS

Assessment of *Gcg* Knockdown

Following euthanasia, the small intestine was removed, flushed with PBS and divided into four equal sections: the first quarter was defined as duodenum, the second quarter, jejunum and the final quarter defined as ileum. *Gcg* expression was also assessed in brainstem, pancreas and colon. Total RNA was isolated from the tail of the pancreas, the first 1 cm piece of each intestinal section (for duodenum, jejunum and proximal ileum), the last 1 cm piece (ileum/distal ileum), or from the proximal half of the colon. Total RNA was extracted from tissues using Tri Reagent (Molecular Research Center, Cincinnati, OH). cDNA was synthesized from DNase I-treated (Thermo-Fisher Scientific, Markham, ON) total RNA (2 μg) using random hexamers and Superscript III (Thermo-Fisher Scientific, Markham, ON). Real-time PCR was carried out using a QuantStudio 5 System and TaqMan Gene Expression Assays (Thermo-Fisher Scientific, Markham, ON). Primer-probe sets were manufactured by Taqman Assays-on-Demand (Applied Biosystems) to measure Exons 1-2 of proglucagon (*Gcg*: Mm01269053_m1), Exons 3-4 of Gastric Inhibitory Polypeptide (*Gip*: Mm00433601_m1). Relative RNA expression was normalized to levels of ribosomal protein L32 (*Rpl32*), or cyclophilin (*Ppia*) mRNA.

Glucose Tolerance Testing

Mice were fasted overnight (~16 h) and oral or intraperitoneal glucose tolerance tests (OGTT or IPGTT, respectively) were carried out using 1.5 g/kg body weight of glucose (15% solution). Blood glucose levels were assessed in tail vein blood using a hand-held glucometer (Contour glucometer, Bayer Healthcare, Toronto, ON). In accordance with animal protocol guidelines regarding blood volumes collected per mouse in a given experiment, blood was collected at either 0, and 5, or 10 minutes (for GLP-1, insulin and GIP), or 0, 15, 30 and 60 minutes (for insulin and glucagon) after glucose administration in heparin-coated capillary microvette tubes. For measurement of total or active GLP-1, insulin, total GIP, and glucagon, blood was mixed with 10% TED (vol/vol) (5,000 KIU/ml Trasylol, 1.2 mg/ml EDTA and 0.1 nmol/l Diprotin A) and plasma was isolated after centrifugation (13,000 rpm 5 min 4°C) and stored at -80°C until further analysis.

Metabolic Measurements

Insulin (#80-INSMSU-E01, Alpco, Salem, NH), glucagon (#10-1281-01, Mercodia, Winston Salem, NC), total GIP (#81517, Crystal Chem, Elk Grove Village, IL), active and total GLP-1 (#K150JWC-1 and #K150JVC-1, Mesoscale, Rockville, MD) were measured in plasma samples obtained before and 5-60 minutes after glucose administration.

Pancreas Samples

Pancreata samples from six non-diabetic human donors (male donors:18, 18, 20, 35 years of age; female donors: 45, 55 years of age) were obtained through a partnership of Vanderbilt University Medical Center) and Dr. Rita Bottino (Institute of Cellular Therapeutics, Allegheny Health Network, Pittsburgh, PA, USA) working with the International Institute for Advancement of Medicine (IIAM) and the National Disease Research Interchange (NDRI), as previously described (Brissova et al., 2018). Small (< 1 cm) human pancreatic samples were snap-frozen and stored at -80°C until analysis. The Vanderbilt University Institutional Review Board declared that studies on de-identified human pancreatic specimens do not qualify as human subject research.

Pancreas-reactivated ($GcgRA^{\Delta PDX1Cre}$), intestinal-reactivated ($GcgRA^{\Delta VilCre}$), *Gcg*-null, *Pdx-1-Cre* and *Vil-Cre* control pancreas samples from 28-week-old male mice were kindly provided by Dr. Darleen Sandoval (University of Michigan).

Tissue Peptide Content

To measure tissue GLP-1, glucagon, insulin or GIP content, a 0.5 cm segment of intestine, 20-35 mg murine pancreas tissue, or 6-37 mg human pancreas tissue were homogenized in 500 μl (or 250 μl for human pancreas tissue) of lysis buffer (50 mM Tris HCl (pH 8 at 4°C), 1 mM EDTA, 10% glycerol (wt/vol), 0.02% Brij-35 (wt/vol)) supplemented with protease inhibitors. Peptide levels were measured in homogenates using the above mentioned assays and normalized to protein content (Bradford assay), or tissue weight.

Gastric Emptying

Male mice were subjected to an acetaminophen absorption test to assess the rate of gastric emptying. Following an overnight fast (~16 h), oral administration of a glucose solution (1.5 g/kg BW) containing 1% (w/v) acetaminophen (#A7085, Sigma, Oakville, ON)

was administered at a dose of 100 mg/kg. Blood was collected from the tail vein into heparin-coated tubes before and 15, 30 and 60 minutes after acetaminophen administration as described (Maida et al., 2008). Acetaminophen levels were measured in plasma using an enzymatic-spectrophotometric assay (Acetaminophen-L3K, #506-30, Sekisui Diagnostics, Lexington, MA).

Food Intake

After an overnight fast (~16 h), mice were weighed, singly housed and given a pre-weighed amount of food (RC; 18% kcal from fat, 2018, Harlan Teklad, Mississauga, ON) with free access to water. Food was then weighed after 2, 4, 8 and 24 hours.

Immunohistochemistry

The pancreas was fixed in 10% neutral-buffered formalin and paraffin embedded. Immunohistochemistry was done on 5-μm histological sections, and serial sections were stained for insulin (#ab181547, Abcam, Toronto, ON), or glucagon (#2760S, Cell Signaling, Danvers, MA).

QUANTIFICATION AND STATISTICAL ANALYSIS

Results are expressed as the mean ± SEM. Statistical comparisons were made by ANOVA, followed by a Dunnet or Tukey post-hoc, or by a 2-way ANOVA followed by a Sidak post-hoc, or by Student t test (when only 2 conditions) using GraphPad Prism 7. A p value <0.05 was considered to be statistically significant.

Cell Metabolism, Volume *30*

Supplemental Information

Gut-Proglucagon-Derived Peptides Are Essential for Regulating Glucose Homeostasis in Mice

Youngmi Song, Jacqueline A. Koehler, Laurie L. Baggio, Alvin C. Powers, Darleen A. Sandoval, and Daniel J. Drucker

Figure S1

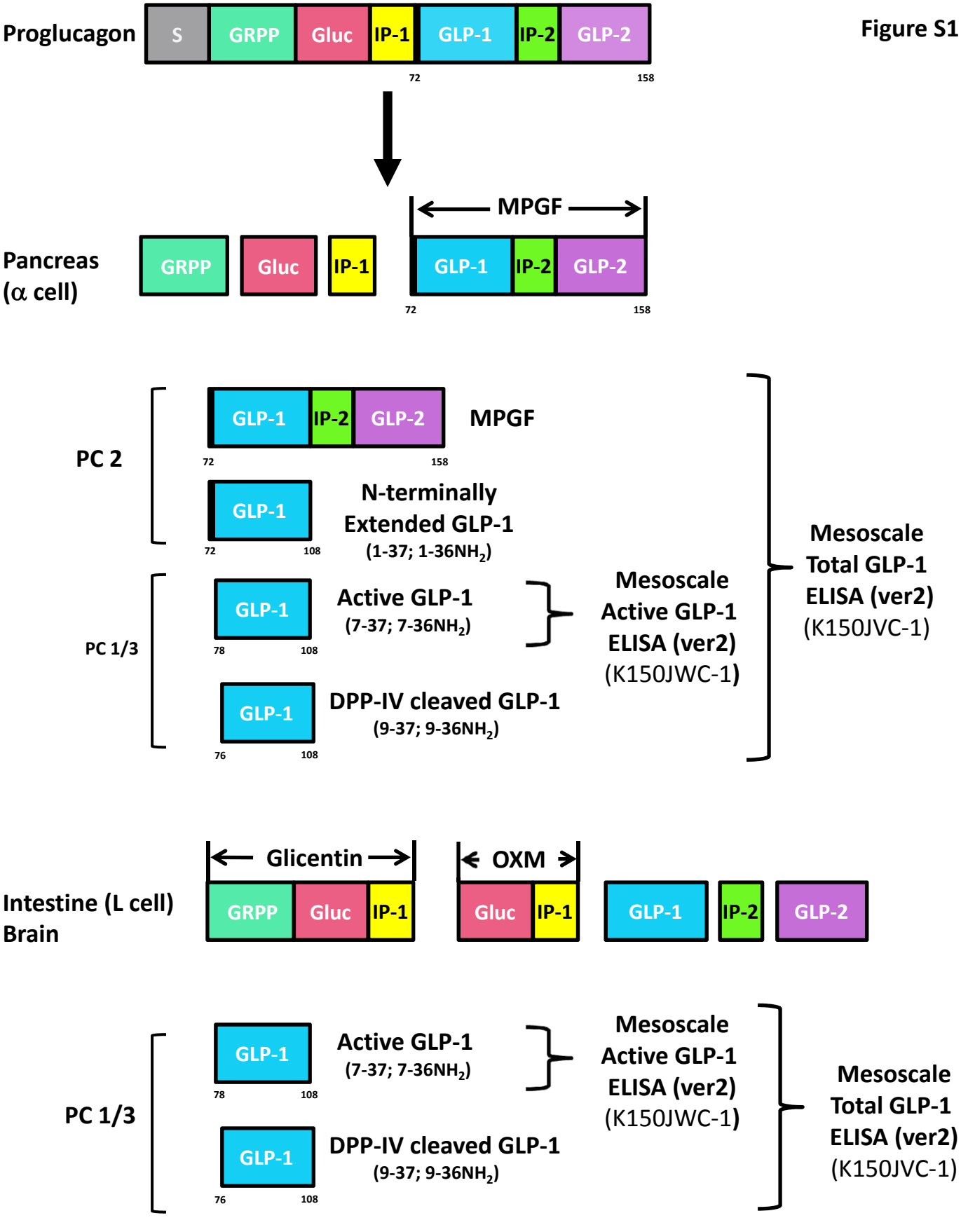
Proglucagon
S
GRPP
Gluc
IP-1
GLP-1
IP-2
GLP-2
72
158
Pancreas
(α cell)
GRPP
Gluc
IP-1
MPGF
GLP-1
IP-2
GLP-2
72
158
PC 2
GLP-1
IP-2
GLP-2
MPGF
72
158
GLP-1
N-terminally
Extended GLP-1
(1-37; 1-36NH2)
72
108
PC 1/3
GLP-1
Active GLP-1
(7-37; 7-36NH2)
78
108
GLP-1
DPP-IV cleaved GLP-1
(9-37; 9-36NH2)
76
108
Mesoscale
Active GLP-1
ELISA (ver2)
(K150JWC-1)
Mesoscale
Total GLP-1
ELISA (ver2)
(K150JVC-1)
Intestine (L cell)
Brain
Glicentin
GRPP
Gluc
IP-1
OXM
Gluc
IP-1
GLP-1
IP-2
GLP-2
PC 1/3
GLP-1
Active GLP-1
(7-37; 7-36NH2)
78
108
GLP-1
DPP-IV cleaved GLP-1
(9-37; 9-36NH2)
76
108
Mesoscale
Active GLP-1
ELISA (ver2)
(K150JWC-1)
Mesoscale
Total GLP-1
ELISA (ver2)
(K150JVC-1)

Figure S1 Related to Figures 1-4: Schematic Representation of Tissue-specific Processing of Proglucagon. In pancreatic α cells, proglucagon is processed by PC 2 into glicentin-related pancreatic polypeptide (GRPP), glucagon (Gluc), the major proglucagon fragment (MPGF), and to some degree to an N-terminally extended form of GLP-1 (1-36NH_2/1-37). In intestinal L cells, proglucagon is cleaved by prohormone convertase 1/3 (PC 1/3) to produce glicentin, oxyntomodulin (OXM), glucagon-like peptide-1 (GLP-1) and GLP-2. Also depicted are the potential products recognized by the two GLP-1 ELISAs utilized in this study. DPP-IV: Dipeptidyl peptidase-4. IP: Intervening peptide.

Figure S2

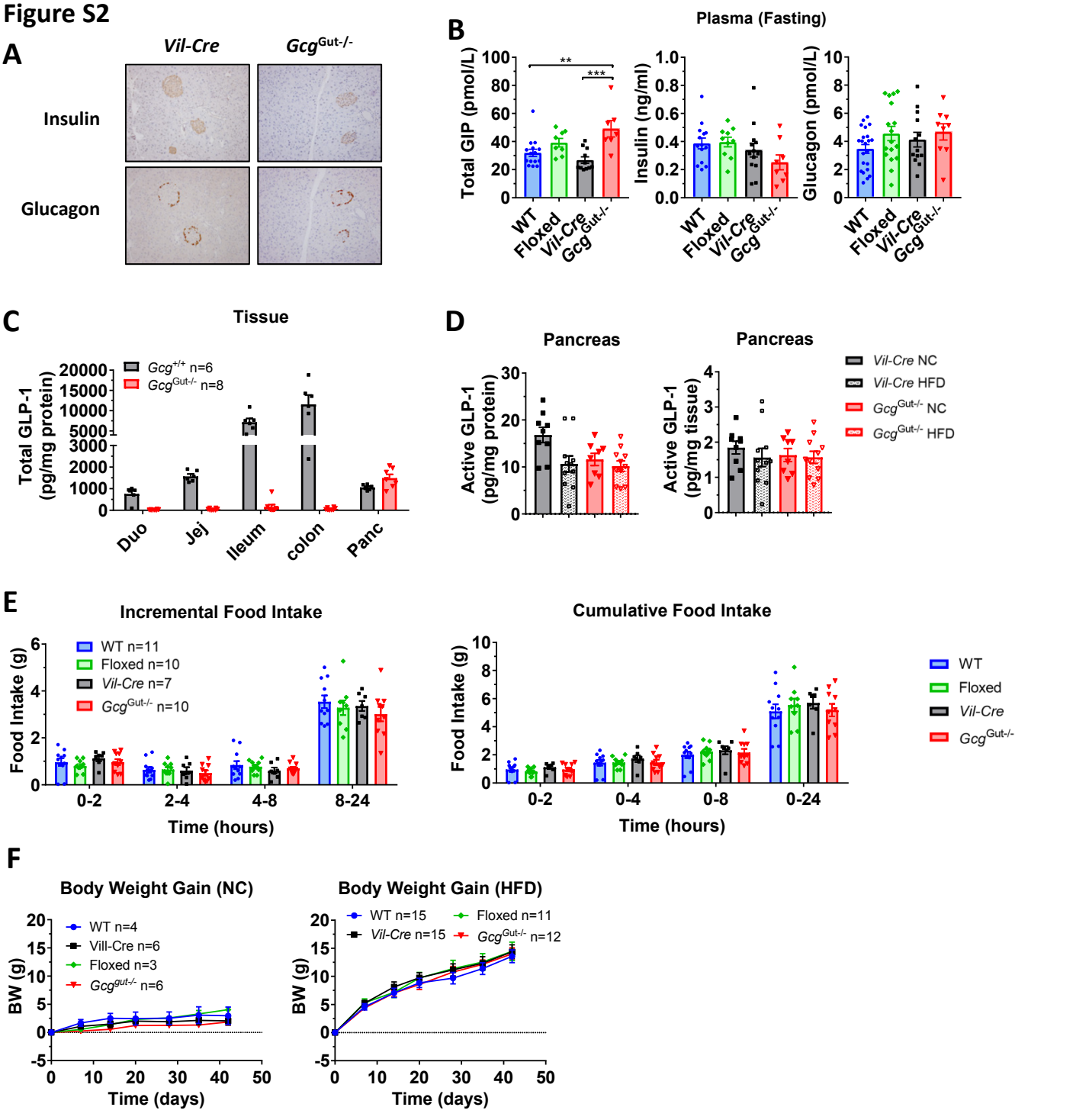

Figure S2 Related to Figures 2 and 3: Glucoregulatory Hormones, Food Intake and Body Weight Gain in *Gcg*$^{Gut-/-}$ mice.
(A) Representative pancreas sections from 22-24-week-old male *Gcg*$^{Gut-/-}$ and *Vil-Cre* control mice stained for insulin or glucagon. (B) Fasting plasma levels of total GIP, insulin and glucagon in 14-17-week-old male *Gcg*$^{Gut-/-}$ and control mice. (n=7-19/group). (C) Total GLP-1 levels, normalized to protein content, in tissue extracts from different regions of the intestine and pancreas of 16-18-week-old female mice. (n=6-8/group).
(D) Active GLP-1 levels, normalized to protein content (*left panel*), or tissue weight (*right panel*), in extracts from pancreas of male *Gcg*$^{Gut-/-}$ and *Vil-Cre* mice fed normal chow (NC), or a 60% high-fat-diet (HFD) for 7 weeks. (n=8-11/group). (E) Incremental (*left panel*) and cumulative (*right panel*) food intake over 24 hours in overnight fasted 11-14-week-old male *Gcg*$^{Gut-/-}$ and control mice.
(F) Weekly body weight gain of male *Gcg*$^{Gut-/-}$ and control mice fed normal chow (NC, *left panel*), or a 60% high-fat-diet (HFD, *right panel*). (n=3-15/group). Data are presented as the mean ± SEM. **p<0.01, ***p=<0.001 *Gcg*$^{Gut-/-}$ *vs.* control mice.

Figure S3

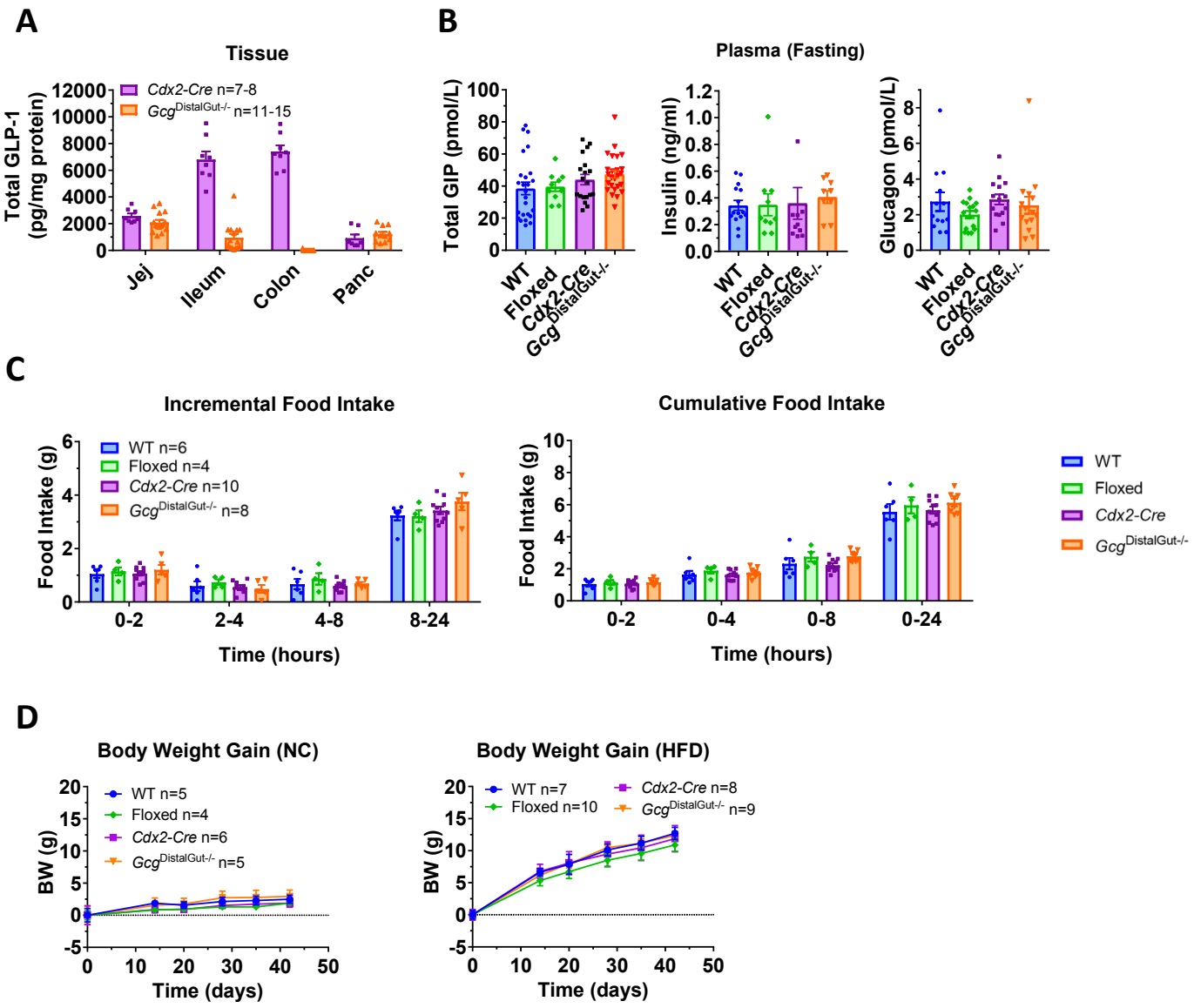

Figure S3 Related to Figure 2 and 4.

Glucoregulatory Hormones, Food Intake and Body Weight Gain in *Gcg*$^{DistalGut-/-}$ mice. (A) Total GLP-1 levels, normalized to protein content, in whole tissue extracts from different regions of the intestine and pancreas of 20-23-week-old male *Gcg*$^{DistalGut-/-}$ and control mice. (n=7-15/group). (B) Fasting plasma levels of total GIP, insulin and glucagon in 10-14-week-old male *Gcg*$^{DistalGut-/-}$ and control mice. (n=5-25/group). (C) Incremental (*left panel*) and cumulative (*right panel*) food intake in overnight fasted 8-week-old male *Gcg*$^{DistalGut-/-}$ and control mice over 24 hours. (n=4-10/group). (D) Weekly body weight gain of *Gcg*$^{DistalGut-/-}$ and control mice fed normal chow (NC, *left panel*), or a 60% high-fat-diet (HFD, *right panel*). (n=3-15/group). Data are presented as the mean ± SEM.

Figure S4

Gcg$^{Gut-/-}$ control mice

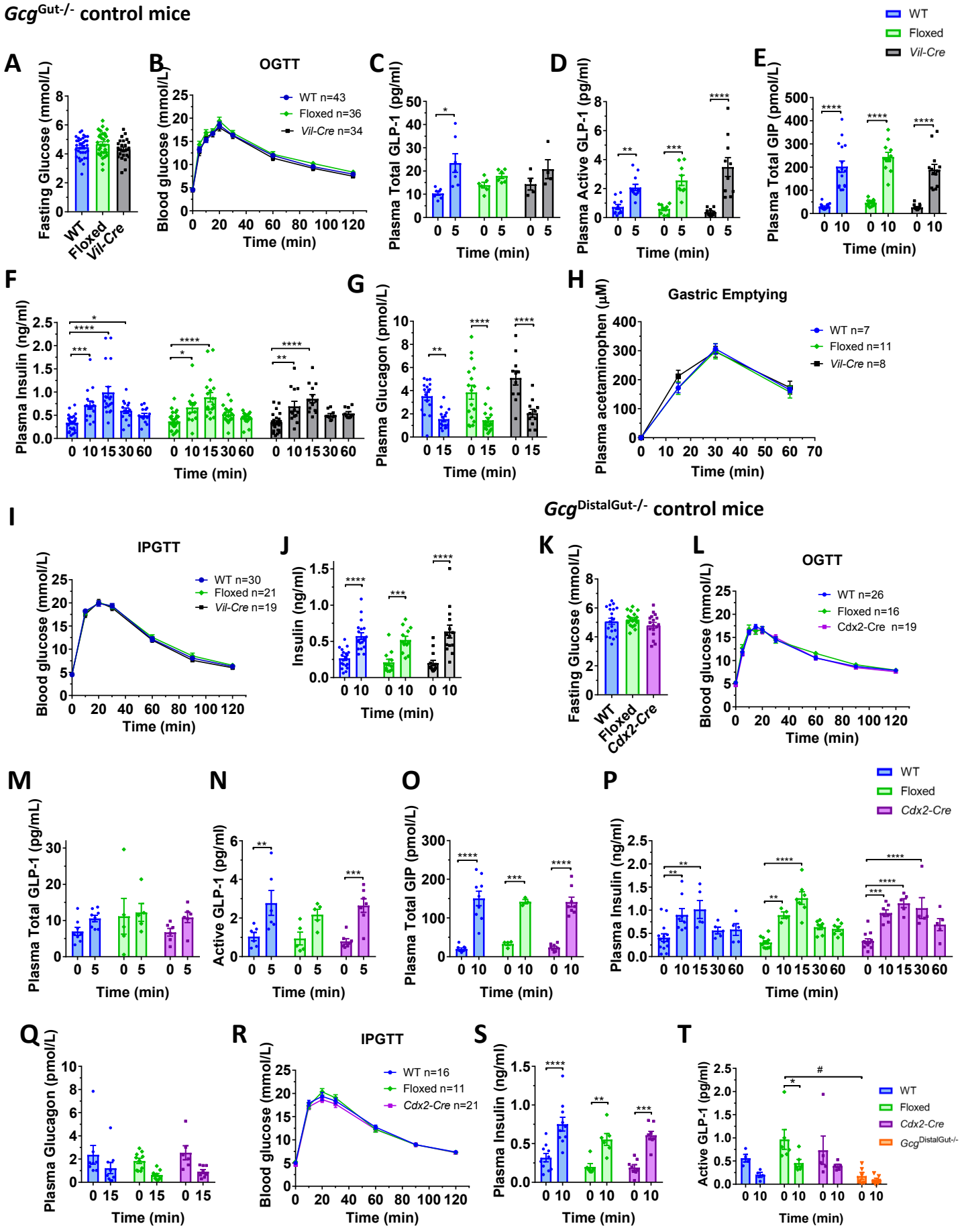

Figure S4 Related to Figures 3 and 4 : Oral and Intraperitoneal Glucose Tolerance in WT, *Gcg*$^{flox/flox}$, *Vil-Cre* and *Cdx2-Cre* Control Mice. (A-B) Fasting glucose and blood glucose levels after oral glucose (1.5g/kg) in overnight fasted 12-17-week-old male *Gcg*$^{Gut-/-}$ control mice. (n=34-43/group). (C) Plasma total GLP-1, (D) active GLP-1, (E) total GIP, (F) insulin, and (G) glucagon measured before and 5-60 min after oral glucose challenge as indicated. (n=4-20/group). (H) Plasma acetaminophen levels, as a measurement of gastric emptying, 0-60 min after co-administration of oral acetaminophen and glucose in overnight fasted 14-17-week-old male *Gcg*$^{Gut-/-}$ control mice. (n=7-11/group). (I) Blood glucose levels taken after intraperitoneal (*i.p.*) administration of glucose (1.5g/kg), and (J) plasma insulin 10 min after *i.p.* glucose challenge in overnight fasted 14-19-week-old male *Gcg*$^{Gut-/-}$ control mice. For (I) n=19-30/group, and (J) n=12-19/group. K-L) Fasting glucose and blood glucose levels after oral glucose (1.5g/kg) in overnight fasted 12-15-week-old male *Gcg*$^{DistalGut-/-}$ control mice. (n=16-26/group). (M) Plasma total GLP-1, (N) active GLP-1, (O) total GIP, (P) insulin, and (Q) glucagon measured before and 5-60 min after oral glucose challenge as indicated. (R) Blood glucose levels taken after intraperitoneal (*i.p.*) administration of glucose (1.5g/kg). (S) Plasma insulin, and (T) active GLP-1 10 min after *i.p.* glucose challenge in overnight fasted 14-17-week-old male control mice (S and T), and *Gcg*$^{DistalGut-/-}$ mice (T). For (R) n=11-21/group and (S) n=6-10/group, (T) n=4-6/group. Data are presented as the mean ± SEM. *p<0.05, **p<0.01, ***p<0.001, ****p<0.0001 basal *vs.* 5-60 min, #p<0.05 *Gcg*$^{DistalGut-/-}$ *vs.* control mice as indicated.

Table S1

Donor Information	1	2	3	4	5	6
Unique identifier	ABGH375	ABHB279	ABI2259	ACEZ011	AFEF080	AFG1440
Donor age (years)	18	18	35	20	55	45
Donor sex (M/F)	M	M	M	M	F	F
Donor BMI (kg/m^2)	31.4	25.1	26.9	19.4	24.2	29.8
Donor HbA_{1c}	N/A	N/A	5.1	5.6	N/A	5.6
Processing center	Pittsburgh	Pittsburgh	VUMC	Vanderbilt	Pittsburgh	Pittsburgh
Donor history of diabetes?	No	No	No	No	No	No
Donor cause of death	Head Trauma / Blunt Injury	Head Trauma / Blunt Injury	Head Trauma / Gunshot wound / Suicide	Head Trauma/Blunt Injury/MVA	Cerebrovascular / Stroke / Intracranial Hemorrhage	Anoxia / Cardiovascular
Warm ischaemia time (h)	N/A	N/A	N/A	N/A	N/A	N/A
Cold ischaemia time (h)	N/A	N/A	N/A	N/A	3.8	9

Table S1 Related to Figure 1

Information related to the human pancreatic samples analyzed in Figure 1. N/A – not available